



## ON THE DYNAMIC CONTACT WITH FRICTION

Ligia Munteanu<sup>1</sup>, Veturia Chiroiu<sup>1</sup>, Cornel Brişan<sup>2</sup>, Dan Dumitriu<sup>1</sup>

<sup>1</sup> Institute of Solid Mechanics, Romanian Academy, Bucharest,

e-mails [ligia\\_munteanu@hotmail.com](mailto:ligia_munteanu@hotmail.com), [veturiachiroiu@yahoo.com](mailto:veturiachiroiu@yahoo.com), [dumitri04@yahoo.com](mailto:dumitri04@yahoo.com),

<sup>2</sup> Technical University of Cluj-Napoca, e-mail [cornel.brisan@mmfm.utcluj.ro](mailto:cornel.brisan@mmfm.utcluj.ro)

**Abstract:** In this paper, the 3D normal vibro-contact problem with friction is investigated for the contact between the tire and the off-road. The road profiles are developed by using the image sonification technique. Direct and inverse approaches for the image sonification are developed in order to determine the contact domain, the natural frequencies and modes when the tire is in ground contact, and also, the pressure distribution of the surface of the half-space which defines the tire tread.

**Keywords:** Vibro-contact; Friction; Tire/off-road contact, Image sonification

### 1. INTRODUCTION

In this work, the dynamic road concept is introduced in order to characterize a particular stretch of road by total longitudinal, lateral, and normal forces as well as their geometric distributions in the contact patches. These forces would give an equivalent driveline which if applied to a contact patch would have the same mechanical effect to the vehicle. For example, if we neglect any slip and if we consider only a point contact, the climbing on a curb or stone with a wheel could be reproduced with a translational couple which can vertically act to raise the wheel. The image sonification is used in this paper to explore the geometric properties of real off-roads with hardly detectable details, or different cross-sectional slices of the image by interpolating the sound parameters furnished by the transformation map.

By applying an inverse algorithm, the analytical representations of the off-roads curves can be developed by using a genetic algorithm. Sonification can be defined as the use of non-speech audio to convey information, possible in a bijective way [1, 2]. The aim of sonification is to turn some sort of data into some sort of sound [3]. General purpose of sonification is the facilitating communication or interpretation of data [4].

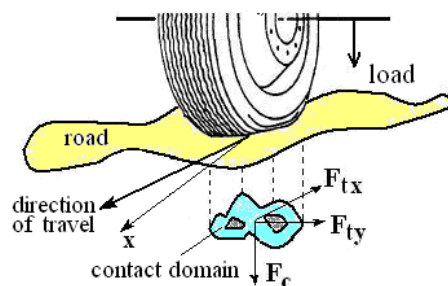


Figure 1: The contact tire/off-road.

Sonification is based on different disciplines ranging from the sciences to the arts, both of which are often linked with technology. As a result, no traditional methods, or canonical form exist for sonification [5].

The sound and vision are interesting and attractive subjects for application of sound in the playback of curve shape and curvature data [6]. In a particular way, they can be designated for driving simulator platforms

A scheme of contact between the tire and the off-road is represented in Figure 1.  $F_c$  is the contact force,  $F_{tx}$  the longitudinal component of the friction force acting in the  $X$  direction,  $F_{ty}$  the lateral component of the friction force acting in the  $Y$  direction.

In this paper, we propose an approach based on the direct and inverse image sonification algorithms, for solving the 3D normal vibro-contact problem with friction for the contact tire/off-road.

## 2. SONIFICATION ALGORITHM

The images chosen for sonification are those of various off-roads. These images depict abrupt changes in profile and can benefit from the accompanying sound by calculating of several cross-sectional slices of them, or even by providing additionally information to that gained from images alone. By using sonification, sounds will be generated directly from digital images, possible in a bijective way, and tested to see whether they aid in the study of them, or not. Cross-sectional slices of the image can be built by interpolating the sound parameters furnished by the transformation map. The aim of sonification is to create a road design algorithm as previously mentioned in [7-9].

A 3D sample of the virtual off-road is represented in Figure 2. The direction of travel is  $OX$ , while the depth of the road is  $OZ$ . Possible 2D  $(X,Y)$  cross-sectional slice of this virtual off-road, before and after deformation, are delimited by two plane curve  $s_1(Z, X)$  and  $s_2(Y, X)$  that can be represented as series of cnoidal functions

$$s_1(Z, X) = \sum_{j=1}^N \alpha_j \text{cn}^j(m_j, k_{1j}X + k_{3j}Z), \quad s_2(Y, X) = \sum_{j=1}^N \beta_j \text{cn}^j(m_j, k_{1j}X + k_{2j}Y), \quad (1)$$

where  $N$  is the finite number of degrees of freedom of the curves,  $0 \leq m_j \leq 1$  is the modulus of the Jacobean elliptic function, and  $\alpha, \beta, k$  are unknown parameters that are determined from an inverse technique.

Consider the set  $D\{d_i, i=1, \dots, M\}$  of sound parameters obtained by applying the sonification operator  $S$  to the virtual off-road shown in Figure 2

$$D = S(p), \quad (2)$$

where  $S(p): \Omega_1 \rightarrow \Omega_2$  is a nonlinear differentiable operator, and  $\Omega_1, \Omega_2$  are open and bounded subset of  $R^n$ .  $\Omega_1$  is an open bounded subset of  $R^n$  representing the set of image data, and  $\Omega_2$  is an open bounded subset of  $R^n$  representing the set of sound data. Consider the inverse nonlinear ill-posed operator equation

$$S^{-1}(D) = s, \quad (3)$$

where  $S^{-1}(D): \Omega_2 \rightarrow \Omega_1$ , and  $s$  ( $s_1(Z, X)$  or  $s_2(Y, X)$ ) is the curve of the cross-sectional slice of the image. Suppose that (3) has at least one solution  $s\{p_i, i=1, \dots, P\}$ . The problem (3) is an ill-posed problem in the sense that the solution of (3) does not depend continuously on data. Almost always only noisy data are available in practice, so that a direct inversion of noise-contaminated data  $D^\delta$  would not lead to a meaningful solution. This article uses a genetic algorithm for recovering of the unknown solution  $s$  of (3) from a noisy version  $D^\delta$  which verifies  $S^{-1}(D^\delta) = s$ . The noisy data  $D^\delta$  with noise level  $\delta$  verify  $\|D^\delta - D\| \leq \delta$ .

The purpose of the inverse problem is to find the parameters

$$P = \{\alpha_j, \beta_j, m_j, k_{1j}, k_{2j}, k_{3j}, \omega_n\}, \quad j = 1, \dots, N, \quad (4)$$

by a least-squares optimization technique. The objective function  $J(P)$  is defined as the distance between the computed data  $p(u)$  for a fixed location of a point belonging to  $s_1(Z, X)$  and/or  $s_2(Y, X)$ , and the corresponding sound data  $D\{d_i, i=1, \dots, M\}$ . The function  $J(P)$  can be expressed as

$$J(P) = \int_C |p(u) - d(u)|^2 ds, \quad (5)$$

A genetic algorithm is used to minimize  $J(P)$ . The genetic algorithm is running until it is reached a non-trivial minimizer  $s(P)$ , which will be a point at which (5) admits a global minimum.

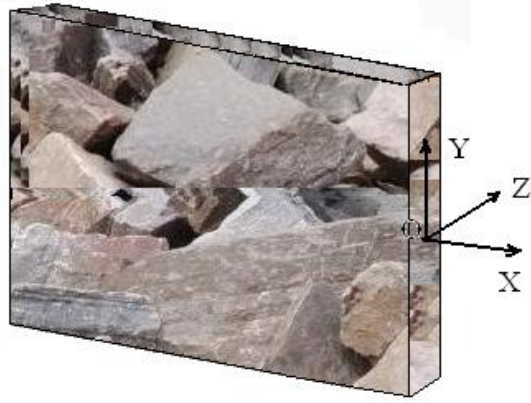


**Figure 2:** A 3D sample of the virtual off-road.

For a cross-sectional slice  $(Z, X)$  of the off-road displayed in Figure 3, the spectra plotted data is represented in the left-hand side of Figure 3, before deformation. It is shown each spectrometer pixel in the range 300 nm to 1000 nm, each pixel is 3.125 nm wide. The absolute amplitudes between plots are not significant. In the right-hand side of Figure 3, the corresponding curve  $s(Z, X)$  before deformation is represented.

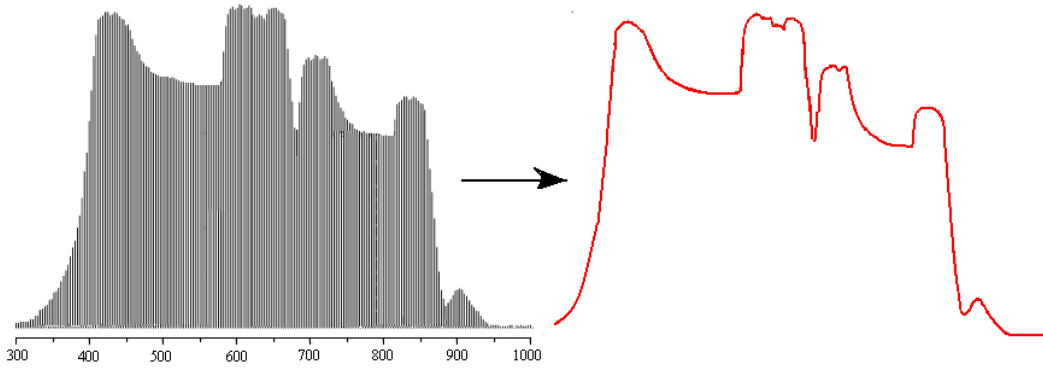


**Figure 3:** Spectra of the cross sectional slice  $(Z, X)$ , and the corresponding curve  $s(Z, X)$  before deformation.

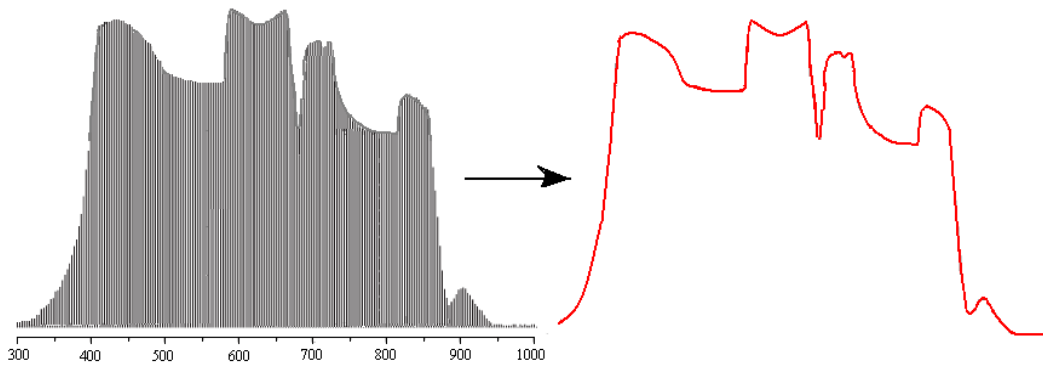


**Figure 4:** Spectra of the cross sectional slice  $(Z, X)$ , and the corresponding curve  $s(Z, X)$  after deformation.

Measurement noise is artificially introduced for determining the curve  $s(Z, X)$  after deformation. It is done by multiplication of the data values for the curve  $s(Z, X)$  before deformation by  $1+r$ ,  $r$  being random numbers uniformly distributed in  $[-\varepsilon, \varepsilon]$ , with  $\varepsilon = 10^{-1}, 10^{-2}, 10^{-3}$ . Spectra of the cross sectional slice  $(Z, X)$ , and the corresponding curve  $s(Z, X)$  after deformation are shown in Figure 4 for  $\varepsilon = 10^{-1}$ .

To shape of the unknown contact domain is taken as a superellipse defined by a Lamé curve [10-13]

$$\left(\frac{x}{a(t)}\right)^n + \left(\frac{y}{b(t)}\right)^n = 1, \quad n > 0, \quad (6)$$

where  $x$  and  $y$  define the envelope of the contact area,  $a$  is half of the contact length, and  $b$  is half of the contact width (radii of the oval shape are depending of time), and  $n$  the power of the ellipsoid.

A representation of in polar coordinates  $x = r \cos \theta$ ,  $y = r \sin \theta$ , is given by

$$r(\theta) = \left[ \left| \frac{\cos \theta}{a} \right|^n + \left| \frac{\sin \theta}{b} \right|^n \right]^{-1/n}, \quad 0 \leq \theta < \frac{\pi}{2}, \quad (7)$$

with  $r = \frac{\tilde{r}}{\max(a,b)}$ ,  $0 \leq r \leq 1$ ,  $\tilde{r} = \left[ \frac{1}{n}(a^n + b^n) \right]^{1/n}$ ,  $\lim_{n \rightarrow \infty} \tilde{r} = \max(a,b)$ . By applying the Sneddon dual integral equations for elastic contact problem [11], the solution of the contact problem can be written as

$$p(r(\theta)) = \left[ \frac{3PH^2E}{2(1-\nu^2)} \right]^{-1/3} \left( \frac{1}{2\bar{E}(\varphi, \bar{k})} \right)^{2/3} (1-r^2\bar{k}^2)^{1/6}, \quad (8)$$

where  $H = \frac{1}{n} \left( \frac{1}{\rho_1} + \frac{1}{\rho_2} \right)$  is the mean curvature of the contact domain  $z = \frac{1}{n} \left( \frac{x^n}{\rho_1} + \frac{y^n}{\rho_2} \right)$ , with  $\rho_1$  and  $\rho_2$  are the

curvature radii in origine.,  $\varphi = \arcsin(1-r)$ ,  $\varphi \leq \frac{\pi}{2}$ ,  $\bar{k} = \frac{(n\tilde{r}^n - 2b^n)^{1/n}}{a}$ ,  $a = \max(a,b)$ , and  $F(\varphi, \bar{k})$ ,

$\bar{E}(\varphi, \bar{k})$  are the elliptic integrals of the first and of the second kind, respectively. The maximum value of  $p(r)$  is obtained for  $r \rightarrow 0$   $\left( \varphi = \frac{\pi}{2} \right)$

$$p_{\max} = p(0) = \left[ \frac{3PH^2E}{(1-\nu)} \right]^{-1/3} \left( \frac{1}{2\bar{E}(\pi/2, \bar{k})} \right)^{2/3} (1-\bar{k}^2)^{1/6}. \quad (9)$$

The displacement  $\delta$  at the surface of the half-space is expressed as

$$\delta_z = \left[ \left( \frac{3}{2} \right)^2 \frac{(1-\nu)^2}{4\pi^2 E^2} P^2 H \right]^{1/3} \frac{(1-\bar{k}^2)^{1/3} K(\bar{k})}{\bar{E}^{1/3}(\bar{k})}. \quad (10)$$

where  $F(\pi/2, \bar{k}) = K(\bar{k})$  and  $\bar{E}(\pi/2, \bar{k}) = \bar{E}(\bar{k})$  are the complete elliptic integrals of the first and of the second kind, respectively, given by

$$c = \ln \left( \tan \left( \frac{3\pi}{8} \right) \right), \quad d = \left( 4^{1/4} c \frac{2\pi P}{l} \frac{\Gamma \left( \frac{1}{2} + \frac{1}{4} \right)}{\Gamma \left( 1 + \frac{1}{4} \right)} \right)^{1/3}. \quad (11)$$

We consider now the same 3D sample of the virtual off-road represented in Figure 2. For arbitrary four cross-sectional slices ( $Z, X$ ) of the off-road, the corresponding vertical displacements  $s_j(t)$ ,  $j = 1, 2, 3, 4$  of tires, are represented in Figure 5.

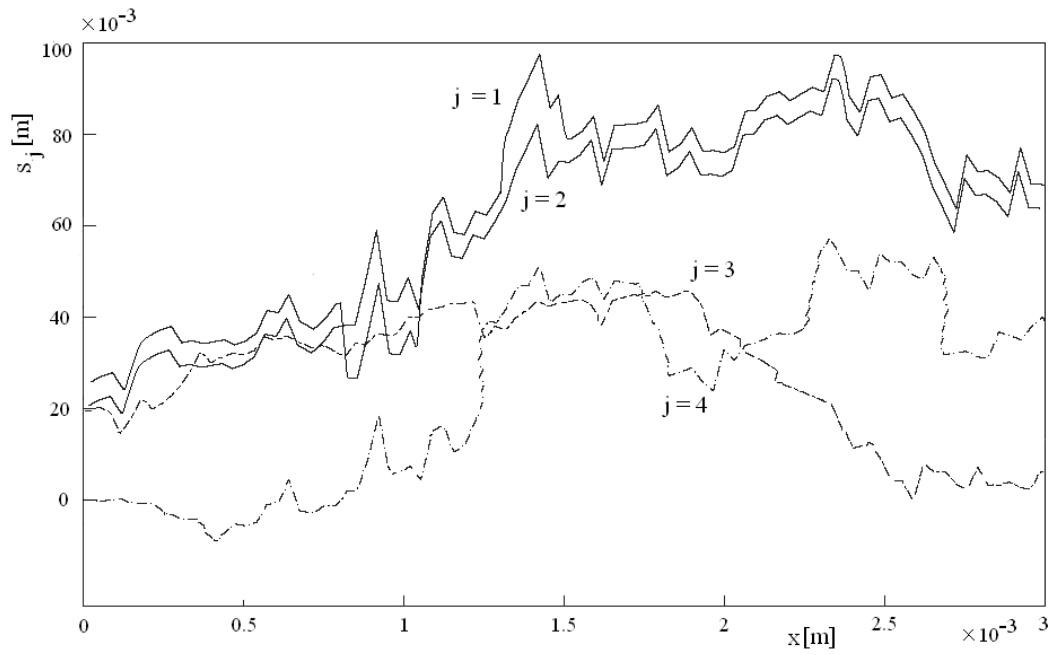


**Figure 5:** Functions  $s_j$ ,  $j = 1, 2, 3, 4$  of vertical displacements of tires in the plane  $(Z, X)$ .

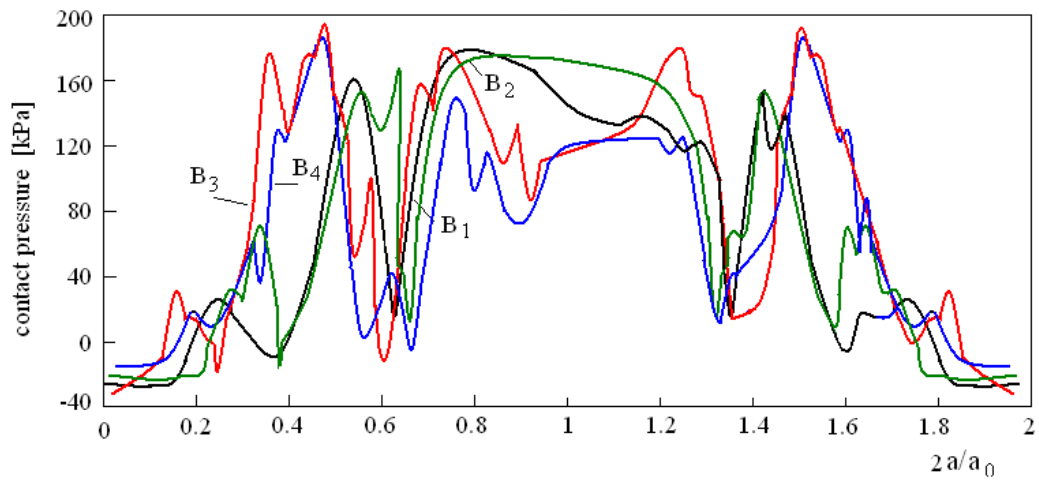


**Figure 6:** Maximum contact pressure in arbitrary contact patch.

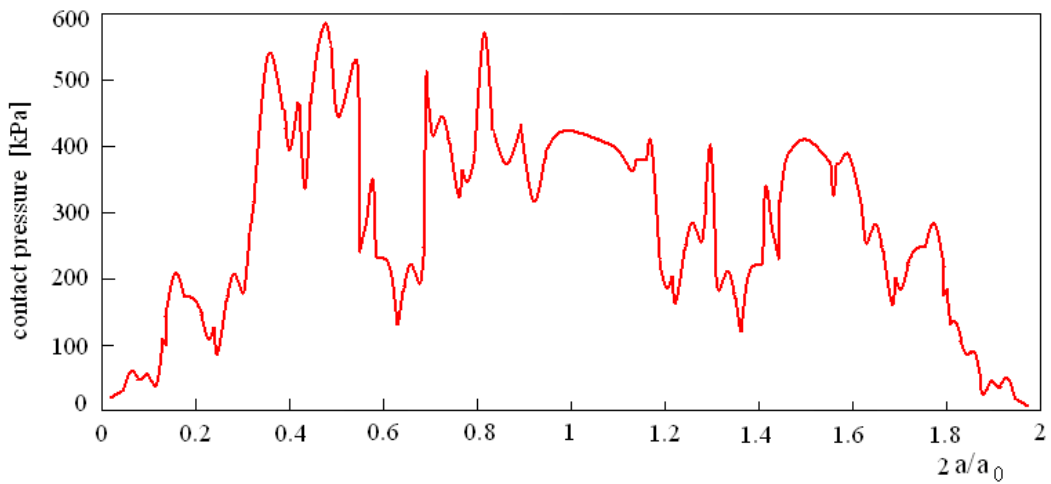


**Figure 7:** Maximum contact pressure in the contact patch.

To compare our results, consider the experiment done to the automotive laboratory of the Mechanical Engineering Faculty, Technische Universiteit Eindhoven with a real car wheel on the flat-plate [14]. After that the pressure is kept constant for approximately 5 seconds and next the pressure is released in 5 seconds. The maximum pressure is 4000 N. Maximum value of the contact pressures for this contact patch with respect to  $2a/a_0$  are plotted in Figure 7, where  $a_0$  is one reference radius of the contact domain. The results are in a perfect agreement with the pressure distribution obtained from experiment.

### 3. CONCLUSION

The aim of this work is to present a virtual experiment concerning the driving on the off-roads, via the building of the road profiles by direct and inverse sonification algorithms. The feasibility of communicating geometrical data through sonification can be useful to build a low-cost virtual reality environment with an increased degree of realism for driving simulators and higher user flexibility. The results are encouraging since they suggest that humans, previously unexposed to the system, are capable of establishing a clear connection between the sound and the underlying data.

**Acknowledgement.** This research was elaborated through the PN-II-PT-PCCA-2011-3.1-0190 Project nr. 149/2012 of the National Authority for Scientific Research (ANCS, UEFISCDI), Romania. The authors acknowledge the similar and equal contributions to this article.

### REFERENCES

- [1] Munteanu, L., Chiroiu, V., Brişan, C., Dumitriu, D., Sireteanu, T., Petre, S., *On the 3D normal tire/off-road vibro-contact problem with friction*, Mechanical Systems and Signal Processing, 2014.
- [2] Kramer, G., *An introduction to auditory display*. In: Kramer G (eds) In auditory display. pp 1–79 Addison-Wesley, Boston, MA, 1994.
- [3] Hermann, T., *Taxonomy and definitions for sonification and auditory display*. Proceedings of the 14th International Conference on Auditory Display, Paris, France June 24 – 27, 2008.
- [4] Bonebright, T., Cook, P., Flowers, J. H., *Sonification Report: Status of the Field and Research Agenda*, Faculty Publications, Department of Psychology, Paper 444, 2010.
- [5] Licht, A., *Sound art, beyond music, between categories*. Rizzoli International Publications, Inc., New York, NY, 2007.
- [6] Shelley, S., Alonso, M., Hollowoof, J., Pettitt, M., Sharples, S., Hermes, D., Kohlrausch, A., *Interactive sonification of curve shape and curvature data*, In Lecture Notes in Computer Science 5763, Haptic and Audio Interaction Design, 4<sup>th</sup> International Conference, HAID2009, Dresden, Germany, Sept 10-11, 2009 (eds. M.Ercan Altinsoy, Ute Jekosch, Stephen Brewster) 51-60, 2009.
- [7] Brişan, C., Vasîu, R.V., Munteanu, L., *A modular road auto-generating algorithm for developing the road models for driving simulators*. Transportation Research part C: Emerging Technologies, 26, 269-284, 2013.
- [8] Vasîu, R.V., Brisan, C., *Aspects regarding modular road design in virtual reality*. In: Proceedings of WINVR, Milan, 27–29 June 2011.
- [9] Vasîu, R.V., Melinte, O., Vlădăreanu, V., Dumitriu, D., *On the response of the car from road disturbances*. Romanian Journal of Technical Sciences – Applied Mechanics, 58(3), 2013.
- [10] Dumitriu, D., Munteanu, L., Brişan, C., Chiroiu, V., Vasîu, R. V., Melinte, O., Vlădăreanu, V., *On the continuum modeling of the tire/ road dynamic contact*. CMES: Computer Modeling in Engineering and Sciences, Materials & Continua, 94 (2), 159-173, 2013.
- [11] Dumitriu, D., Chiroiu, V., *On the dual equations in contact elasticity*. Revue Roumaine des Sciences Techniques – Série de Mécanique Appliquée, 2006.
- [12] Munteanu, L., Brişan, C., *On the modeling of contact interfaces with frictional slips*, Analele Universităţii “Eftimie Murgu” Reşiţa, Fascicola de Inginerie, XX(2), 17-24, 2013.
- [13] Munteanu, L., Brisan, C., Chiroiu, V., Donescu, Şt., *A 3D model for tire/road dynamic contact*. Acta Technica Napocensis, Series: Applied Mathematics and mechanics, 55(3), 611–614, 2012.
- [14] Backs, P.W., *Tyre/road contact measurements using pressure sensitive films*. Technische Universiteit Eindhoven, Report DCT 2007-026, 1-35, 2007.